Dynamics of Cracked Composite Shafts

A. S. Sekhar and B. N. Srinivas

Journal of Reinforced Plastics and Composites 2003 22: 637
DOI: 10.1177/073168403029358

Dynamics of Cracked Composite Shafts

A. S. SEKHAR* AND B. N. SRINIVAS
Department of Mechanical Engineering
Indian Institute of Technology
Kharagpur – 721 302, India

ABSTRACT: The dynamics of cracked rotors has been the study for the last three decades. However, considering the importance in the practical fields, the vibration characteristics of cracked rotors are still under active investigation. It needs more attention, particularly with the emerging of new materials such as composites for shafts. The present study aims at the analysis of the cracked composite shafts. The composite shaft has been modelled based on first order shear deformation theory using finite element method with shell elements. Different materials such as, boron–epoxy, carbon–epoxy and graphite–epoxy have been tried for various stacking sequences. The influences of crack parameters, fibre orientation (stacking sequences) and material properties on the vibration characteristics of composite shafts have been studied.

KEY WORDS: cracks, composite shaft, stacking sequence, finite elements.

INTRODUCTION

THE DYNAMIC BEHAVIOUR of structures – in particular rotors containing cracks is a subject of considerable interest for the last three decades after the first studies were started by Dimarogonas [1]. The review of the investigations on this subject can be seen in [2–5]. However, all the works reported in [1–5] consider mainly isotropic beams/shafts.

With the emerging of new materials such as composites for shafts, the early detection of the crack initiation and predication of its growth become important to avoid catastrophic failure. Composite materials have many advantages, which made them applicable to a wide variety of products. The high specific stiffness and specific strength of composite materials made

*Author to whom correspondence should be addressed. E-mail: sekhar@mech.iitkgp.ernet.in

0731-6844/03/07 0637–17 $10.00/0 DOI: 10.1177/073168403029358

them very useful. Because of these advantages, attempts have been made to replace isotropic shafts with composite shafts.

Several investigations are reported on composite beams. To name a few, Karabalis and Bexos [6] have studied static, dynamic, and stability analysis of structures composed of tapered beams while Abramovich and Livshits [7] have done free vibration of non-symmetrically laminated cross ply composite beams based on Timoshenko type equations. Kim and Green [8] have studied the sensitivity of the modal damping and natural frequencies of adhesively bonded and composite beams to small pre-deformations. Dynamic analyses of beams have been studied by Chen and Mucino [9] while Ramalingeswara Rao and Ganesan [10] included tapered beams also. Damage analyses such as cracks have also been investigated in composite beams by Krawczuk and Ostachowicz [11].

There has been limited research work on composite shafts even though, way back Zinberg and Symmonds [12] have done on composites. The Equivalent Modulus Beam Theory (EMBT), as used by them has the following defects: (i) it does not account for the bending and stretching coupling and shear normal effects; (ii) the shear of the tube cannot be accurately represented; (iii) the cross sectional deformations as well as out of plane warping are not included. Henriqúe dos et al. [13] predicted critical speeds using Donnell's shell theory. The main drawback in the above theory is that it is difficult to adapt for rotordynamics analysis in which lumped masses, gyroscopic effects and flexible damped bearing are important and necessary conditions.

More recently, Singh and Gupta [14] predicted critical speeds using layerwise theory, which overcome the above defects. Further, they [15] performed experimental investigation to determine damping effects in the material. But this theory involves increased complexity and computation time, the number of equations being dependent on the number of laminae in the laminate.

Influences of imperfections are predicted by Wettergren [16]. Optimal sizing of composite power transmission shafting with the goal of minimising weight was done by Lim and Darlow [17]. The majority of research on composite shafts has been involved in the automobile industry. Belingardi et al. [18] investigated the use of fibre–matrix composite transmission shafts for medium size passenger cars. In order to advance the application of these composites into aerospace field it must be determined for design and practicality. Very recently, Salzar [19] demonstrated the feasibility of using lighter weight/stronger composite shafts as well as the complexity of the design problem along with the careful consideration of practicality that must be taken prior to the abandonment of traditional monolithic designs in highly critical applications. The dynamic aspects of composite shafts for

different material and fibre orientations have been analysed recently, by Sekhar and Ravi Kumar [20] based on the first order shear deformation theory using finite element method.

Based on the discussions on the composite shafts it is essential to analyse the effects of cracks on the dynamics of composite shafts. The present study aims at the finite element analysis of cracked composite shafts for different materials such as, boron–epoxy, carbon–epoxy and graphite–epoxy for various stacking sequences.

MODELLING OF COMPOSITE SHAFT

A hollow composite shaft made of four laminae as shown in Figure 1 is considered. The finite element formulation for the composite shaft is based on the first order shear deformation theory. The modelling as used in [20] is discussed briefly here again. The stress–strain relationship for orthotropic material for a single layer in material principle direction is given as

$$\{\sigma\} = [Q]\{\varepsilon\} \tag{1}$$

$$\{\varepsilon\} = [S]\{\sigma\} \tag{2}$$

where $[Q]$ is the elasticity matrix and $[S]$ is the compliance matrix.

Three-displacement components u, v and w in the direction of x, y and z define the state of displacement of a nodal point as shown in the Figure 2.

$$\{\delta\} = [u \quad v \quad w]^T = \begin{bmatrix} 1 & 0 & 0 & z & 0 \\ 0 & 1 & 0 & 0 & z \\ 0 & 0 & 1 & 0 & 0 \end{bmatrix} \begin{Bmatrix} u_0 \\ v_0 \\ w_0 \\ \theta_x \\ \theta_y \end{Bmatrix} \tag{3}$$

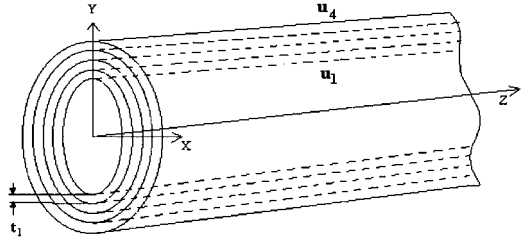

Figure 1. *Composite shaft model.*

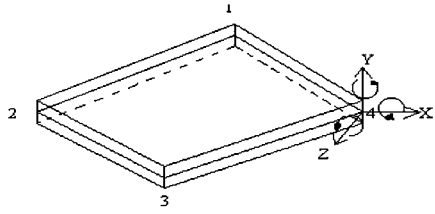

Figure 2. *Four noded shell element.*

$$\{\varepsilon\}^T = \left\{\{\varepsilon_x\}\,\{\varepsilon_y\}\,\{\varepsilon_{xy}\}\,\{\varepsilon_{xz}\}\,\{\varepsilon_{yz}\}\right\} \tag{4}$$

But

$$\varepsilon_x = \bar{S}_{11}\sigma_x + \bar{S}_{12}\sigma_y + \bar{S}_{13}\sigma_z$$

$$\varepsilon_y = \bar{S}_{12}\sigma_x + \bar{S}_{22}\sigma_y + \bar{S}_{23}\sigma_z$$

$$\varepsilon_z = \bar{S}_{13}\sigma_x + \bar{S}_{23}\sigma_y + \bar{S}_{33}\sigma_z$$

where $\bar{S}_{11}, \ldots, \bar{S}_{33}$ are the elements of the compliance matrix referred to geometrical natural axes x–y obtained by transformation of stress–strain relation for generally orthotropic material.

Expressing σ_z in terms of σ_x and σ_y, we can get $[Q]$ matrix

$$\varepsilon_x = \frac{\partial u_0}{\partial x} + z\frac{\partial \theta_x}{\partial x} \tag{5}$$

$$\varepsilon_y = \frac{\partial v_0}{\partial x} + z\frac{\partial \theta_y}{\partial y} \tag{6}$$

$$\varepsilon_{xy} = \left(\frac{\partial u_0}{\partial y} + \frac{\partial v_0}{\partial x}\right) + \left(\frac{\partial \theta_x}{\partial y} + \frac{\partial \theta_y}{\partial x}\right) \tag{7}$$

$$\varepsilon_{xz} = \frac{\partial w}{\partial x} + \theta_x \tag{8}$$

$$\varepsilon_{yz} = \frac{\partial w}{\partial y} + \theta_y \tag{9}$$

$$\begin{Bmatrix} \varepsilon_x \\ \varepsilon_y \\ \varepsilon_{xy} \\ \varepsilon_{xz} \\ \varepsilon_{yz} \end{Bmatrix} = \begin{bmatrix} 1 & 0 & 0 & z & 0 & 0 & 0 & 0 \\ 0 & 1 & 0 & 0 & z & 0 & 0 & 0 \\ 0 & 0 & 1 & 0 & 0 & z & 0 & 0 \\ 0 & 0 & 0 & 0 & 0 & 0 & 1 & 0 \\ 0 & 0 & 0 & 0 & 0 & 0 & 0 & 1 \end{bmatrix} \begin{Bmatrix} \partial u_0/\partial x \\ \partial v_0/\partial y \\ \dfrac{\partial u_0}{\partial y} + \dfrac{\partial v_0}{\partial x} \\ \partial \theta_x/\partial x \\ \partial \theta_y/\partial y \\ \dfrac{\partial \theta_x}{\partial y} + \dfrac{\partial \theta_y}{\partial x} \\ \dfrac{\partial w}{\partial x} + \theta_x \\ \dfrac{\partial w}{\partial y} + \theta_y \end{Bmatrix} \tag{10}$$

$$\{\varepsilon\} = [\bar{Z}]\{\bar{\varepsilon}\} \tag{11}$$

$$\{\bar{\varepsilon}\} = \begin{bmatrix} \dfrac{\partial}{\partial x} & 0 & 0 & 0 & 0 \\ 0 & \dfrac{\partial}{\partial y} & 0 & 0 & 0 \\ \dfrac{\partial}{\partial y} & \dfrac{\partial}{\partial x} & 0 & 0 & 0 \\ 0 & 0 & 0 & \dfrac{\partial}{\partial x} & 0 \\ 0 & 0 & 0 & 0 & \dfrac{\partial}{\partial y} \\ 0 & 0 & 0 & \dfrac{\partial}{\partial y} & \dfrac{\partial}{\partial x} \\ 0 & 0 & \dfrac{\partial}{\partial x} & 1 & 0 \\ 0 & 0 & \dfrac{\partial}{\partial y} & 0 & 1 \end{bmatrix} \begin{Bmatrix} u_0 \\ v_0 \\ w_0 \\ \theta_x \\ \theta_y \end{Bmatrix} \tag{12}$$

$$\{\bar{\varepsilon}\} = [L][N]\{d^e\} = [B]\{d^e\} \tag{13}$$

where L is the linear operator matrix. N is the shape function matrix and B is the strain nodal displacement matrix.

$$[B] = [[B]_1[B]_2, \ldots, [B]_n] \tag{14}$$

$$[B]_i = \begin{bmatrix} \frac{\partial n_i}{\partial x} & 0 & 0 & 0 & 0 \\ 0 & \frac{\partial n_i}{\partial y} & 0 & 0 & 0 \\ \frac{\partial n_i}{\partial y} & \frac{\partial n_i}{\partial x} & 0 & 0 & 0 \\ 0 & 0 & 0 & \frac{\partial n_i}{\partial x} & 0 \\ 0 & 0 & 0 & 0 & \frac{\partial n_i}{\partial y} \\ 0 & 0 & 0 & \frac{\partial n_i}{\partial y} & \frac{\partial n_i}{\partial x} \\ 0 & 0 & \frac{\partial n_i}{\partial x} & 1 & 0 \\ 0 & 0 & \frac{\partial n_i}{\partial y} & 0 & 1 \end{bmatrix} \tag{15}$$

Element stiffness equation is given by

$$\lfloor k^e \rfloor \{a^e\} = \{f^e\}$$

where $\{f^e\}$ is the element nodal point force vector and $[k^e]$ is the element stiffness matrix given by

$$[k^e] = \iiint [B]^T [D][B] dV \tag{16}$$

where $[D]$ is given by

$$[D] = \sum_{L=1}^{m} \int_{h_l}^{h_{l+1}} [\bar{z}]^T [Q][\bar{z}] dz \tag{17}$$

The final governing equation is simply the sum of all element stiffness matrices along with the assembly of load matrices. After inserting appropriate restrained boundary conditions, frontal solution technique is used. The main feature of frontal solution technique is that it assembles the equation and eliminates the variables at the same time.

CRACK MODELLING IN NASTRAN

The composite shaft is modelled using FEMAP, which is used for pre- and post-processing of the model with NASTRAN as the solver. The model is created in the pre-processing stage of the model and the results are viewed in the post-processing stage. The composite shaft is created using shell elements with 4 nodes using CQUAD4 elements. The properties of the laminae are given as inputs using PCOMP property cards.

The cracks in a shaft are generated by using bullion operations. For this, a small strip of negligible thickness of 0.25 mm block is created first, then this block is moved to a position where the crack is to be generated. After that, the strip is removed from the moved position and this will create a crack.

Figures 3(a) and (b) show the discretized model of uncracked and cracked composite shafts. Crack has been considered at 0.6 m from the left end. Using bullion operation as explained earlier a crack is generated. A small block at the centre of the shaft indicates the disc. Mesh is refined around the crack. Around 800 elements are considered for this model. The rotor disc is modelled with concentrated mass and weight of the rotor is transferred to the nodes by using rigid elements. A two-dimensional orthotropic material is used, for the analysis using MAT8 card. The bearings have been modelled as spring elements. These are scalar zero-dimensional elements.

RESULTS AND DISCUSSION

The composite shaft modelling was checked with the previous results [14] and were matching very well as explained in [20].

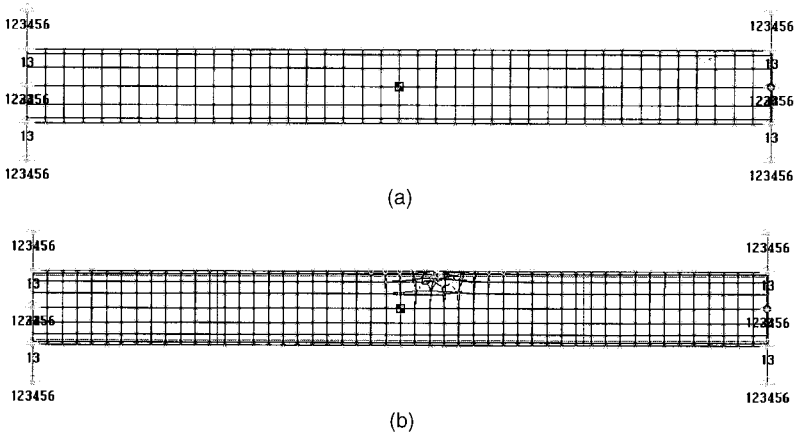

Figure 3. *(a) Composite shaft model without crack; (b) composite shaft model with crack.*

Table 1. Properties of different composite materials.

Material	E_1 (GPa)	E_2 (GPa)	ν_{12}	$G_{12} = G_{13}$ (GPa)	G_{23} (GPa)	ρ (kg/m^3)
Boron–epoxy	211	24.1	0.36	6.9	6.9	1967
Graphite–epoxy	139	11	0.313	6.05	3.78	1578
Carbon–epoxy	130	10	0.25	7.0	7.0	1500

Four layers of equal thickness (0.004 m) with different stacking sequence are considered for the analysis of cracked composite shaft. Parametric study has been done to determine the influences of stacking sequence, material and crack parameters. The properties of the different materials are shown in Table 1. The following data is considered for the analysis of the problem.

Length of the rotor	= 1 m
Radius of the shaft	= 0.05 m
Thickness	= 0.016 m
Material	= Carbon–Epoxy
	= Boron–Epoxy
	= Graphite–Epoxy
Disk mass (located at centre)	= 7 kg
Eccentricity	= 0.01 mm
Lateral moment of inertia	= 0.013 kg/m^2
Polar moment of inertia	= 0.026 kg/m^2
Bearing stiffness	= 10E5 N/m
Damping coefficient	= 0.5

The effects of eigen frequencies are plotted after normalising the crack depth with outer radius (0.05 m). The unbalance response in the y direction is plotted after normalising with maximum response of a shaft of carbon–epoxy at 90/90/0/0 stacking sequence with 0.008 m crack depth.

Effect of Crack on Eigen Frequency

The characteristic difference of cracked composite rotor mode shape with that of uncracked composite rotor is seen in Figures 4(a) and (b). Figures 5 and 6 reveal the effect of crack on first eigen frequency for different fibre orientations and materials. With increase of crack depth eigen frequencies are decreasing. And also the figures show that the shaft of boron–epoxy has higher eigen frequency as compared to that of carbon–epoxy and graphite–epoxy. It can also be seen that the orientation of fibres influences a lot on the eigen frequencies (Figures 5a–c). As can be seen from Figures 6a–c, 90/90/0/0 stacking sequence has higher frequency

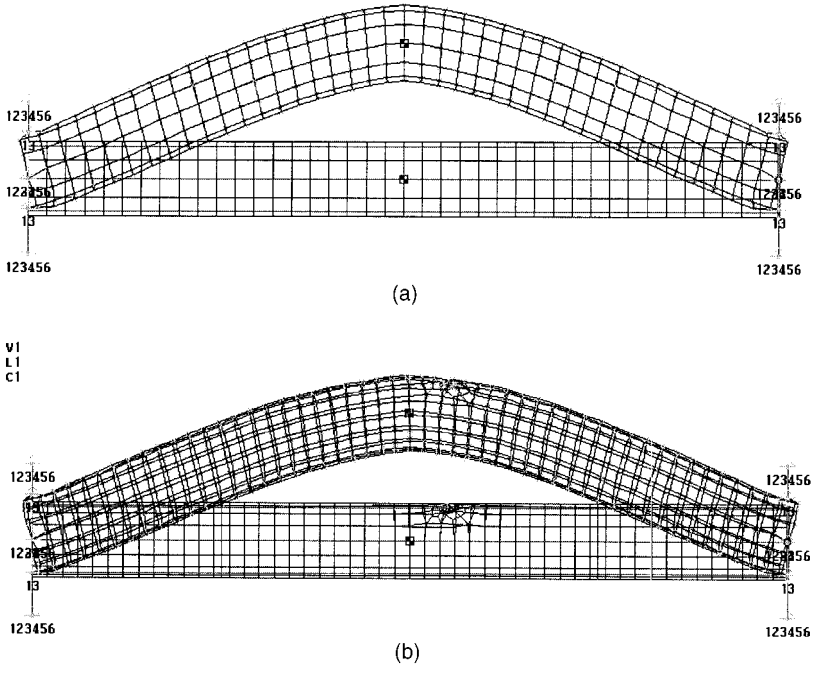

Figure 4. *(a) Mode 1 for composite shaft without crack; (b) mode 1 for composite shaft with crack.*

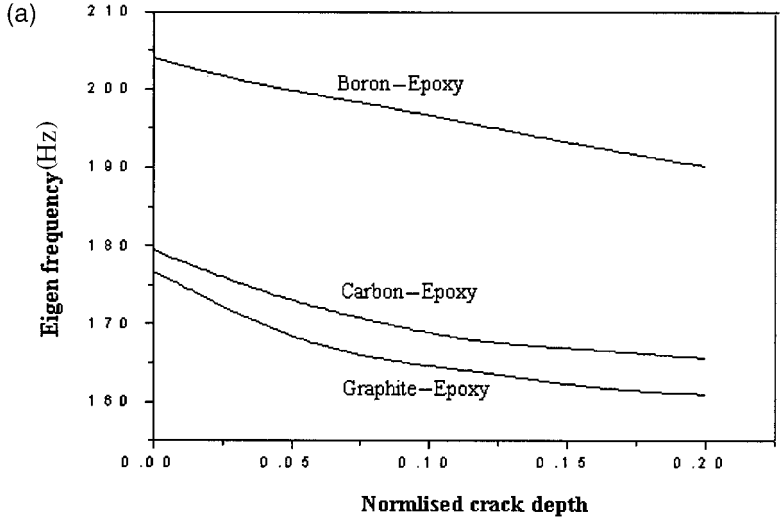

Figure 5. *(a) Effect of crack depth on eigen frequency for different materials (0/0/90/90); (b) effect of crack depth on eigen frequency for different materials (90/90/0/0); (c) effect of crack depth on eigen frequency for different materials (90/0/90/0).*

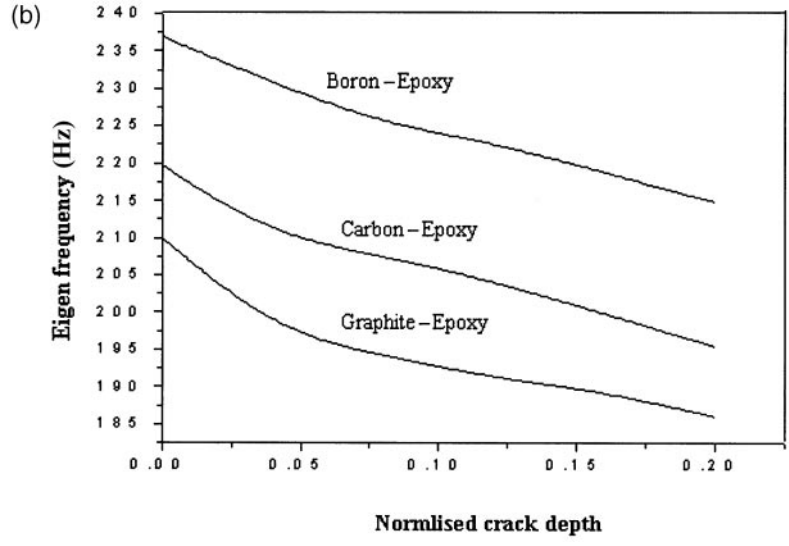

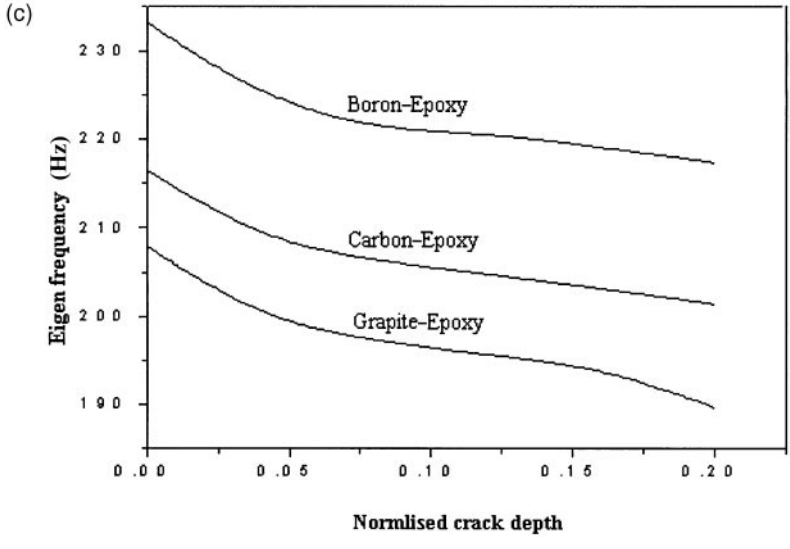

Figure 5. *(Continued).*

at no crack, but when crack depth increases, the eigen frequencies are decreasing at a faster rate as compared to other stacking sequences for all the materials studied. Thus this stacking sequence is very sensitive to crack.

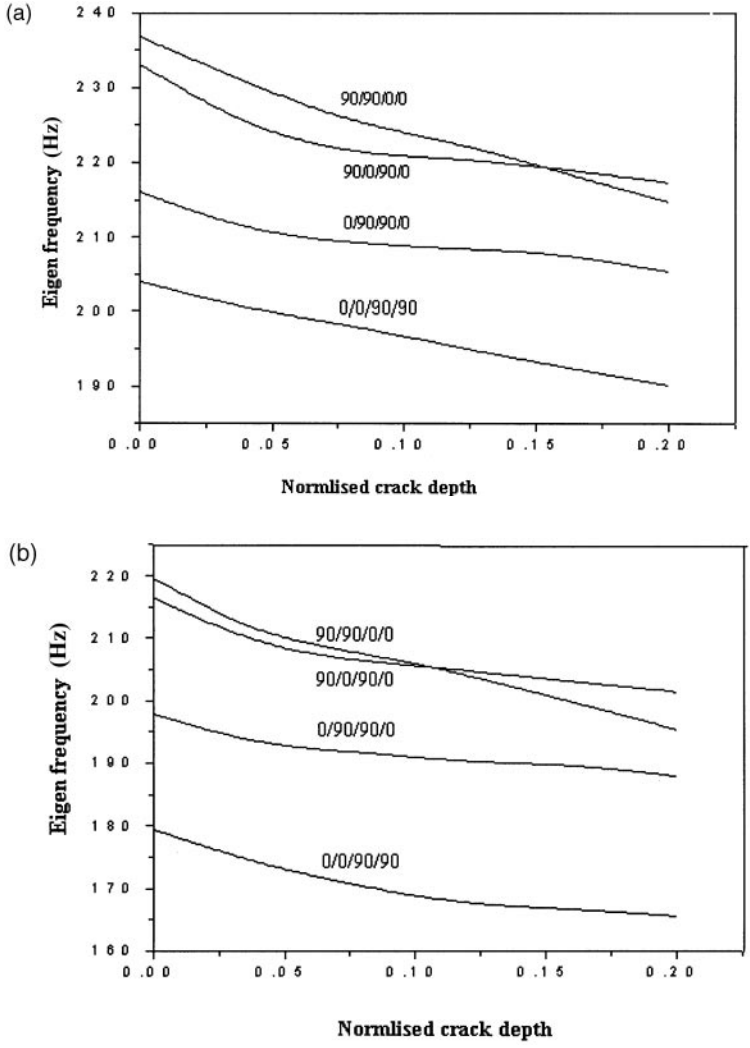

Figure 6. *(a) Effect of crack depth on eigen frequency for boron–epoxy with different stacking sequences; (b) effect of crack depth on eigen frequency for carbon–epoxy with different stacking sequences; (c) effect of crack depth on eigen frequency for graphite–epoxy with different stacking sequences.*

Unbalance Response

To study the response characteristics of a cracked composite shaft, a disc of mass 7 kg with an eccentricity of 0.01 mm is mounted on the shaft at the rotor centre. From the unbalance response, in Figure 7(a), it can be noticed

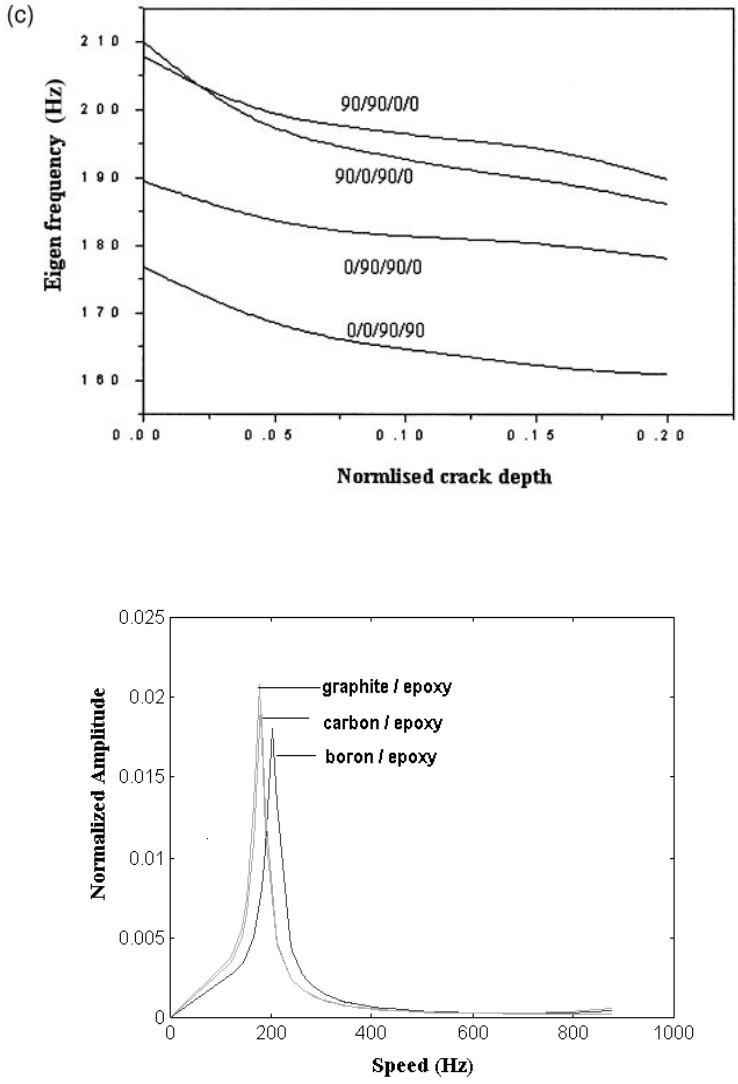

Figure 7. *(a) Unbalance response for different materials at no crack (0/0/90/90); (b) unbalance response for different materials at crack depth 0.004 m (0/0/90/90); (c) unbalance response for different materials at crack depth 0.006 m (0/0/90/90).*

that the boron–epoxy shaft with central disk is stiffer than that of the other materials. Figures 7(b) and (c) show the unbalance response for different materials at different crack depths, for same damping coefficient and same stacking sequence (0/0/90/90).

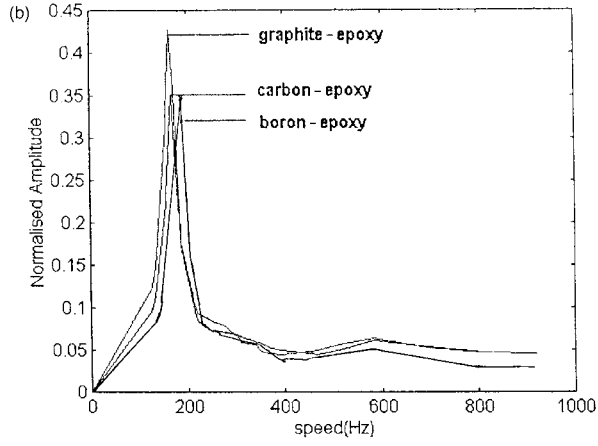

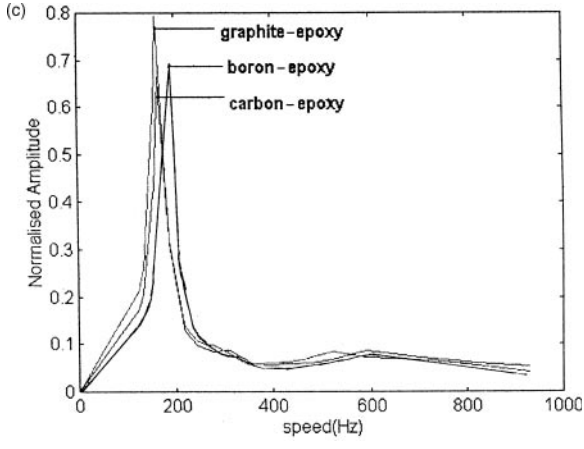

Figure 7. *(Continued).*

Figure 8(a)–(c) also reveals the effect of material at different crack depths and at same stacking sequence. If there is no crack on the shaft, Boron–Epoxy has lower peak amplitude as compared to carbon–epoxy and graphite–epoxy. But with the increase of crack depth, it is observed that the peak amplitude of carbon–epoxy shaft increases at a slower rate as compared to that of boron–epoxy and graphite–epoxy. In all the cases, it can also be observed that if the crack depth increases the peak amplitude shifts towards the lower speed with a raise in amplitude.

The unbalance response for boron–epoxy shaft for different stacking sequences is shown in Figure 9(a) and (b). It can be noted that the critical

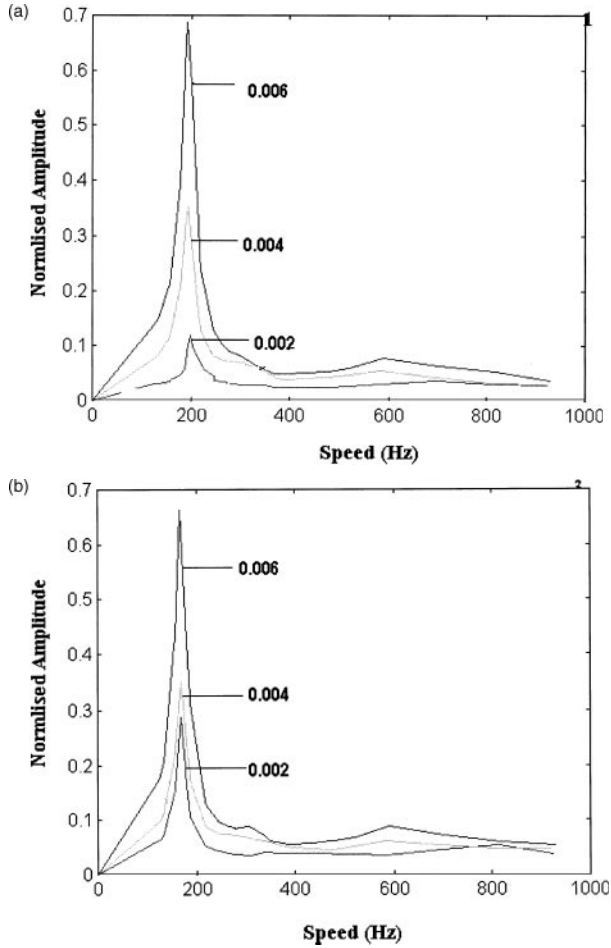

Figure 8. *(a) Unbalance response for boron–epoxy at different crack depths (0/0/90/90); (b) unbalance response for carbon–epoxy at different crack depths (0/0/90/90); (c) unbalance response for graphite–epoxy at different crack depths (0/0/90/90).*

speed of rotor with the 90/0/90/0 is higher compared to other stacking sequences. At higher crack depths the split of critical speeds are also observed in the response plots (Figure 9c).

CONCLUSIONS

The finite element analysis of cracked composite shafts for different materials such as, boron–epoxy, carbon–epoxy and graphite–epoxy for various stacking sequences has been carried out.

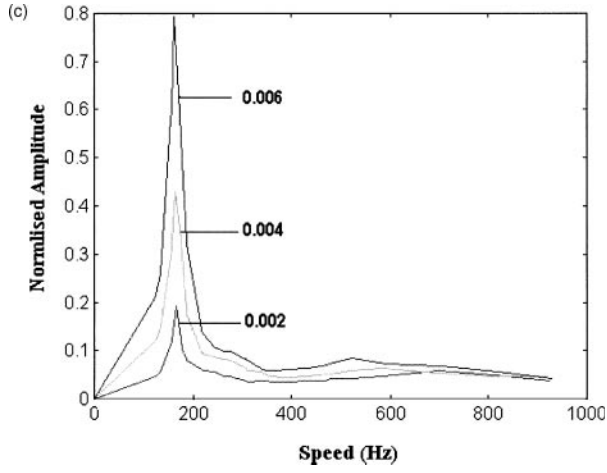

Figure 8. *(Continued).*

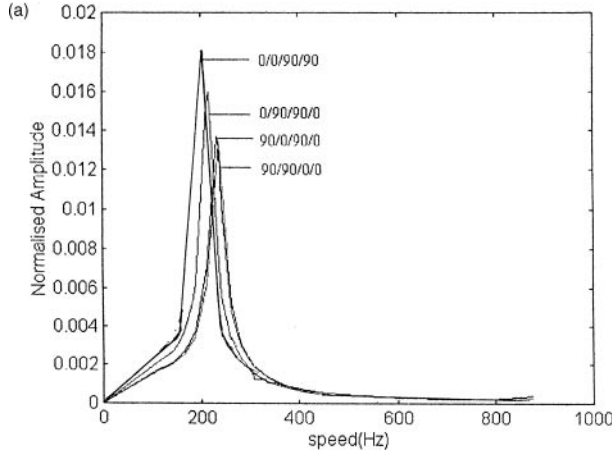

Figure 9. *(a) Unbalance response for boron–epoxy with different stacking sequences at no crack; (b) unbalance response for boron-epoxy with different stacking sequences at crack depth 0.004 m; (c) unbalance response for graphite–epoxy with different stacking sequences at crack depth 0.008 m.*

The influence of crack depth on all the shafts with different materials is more or less same i.e., the eigen frequencies decrease with increase in crack depth. Boron–epoxy shaft has higher frequency compared to that of graphite–epoxy and carbon–epoxy even with the presence of cracks.

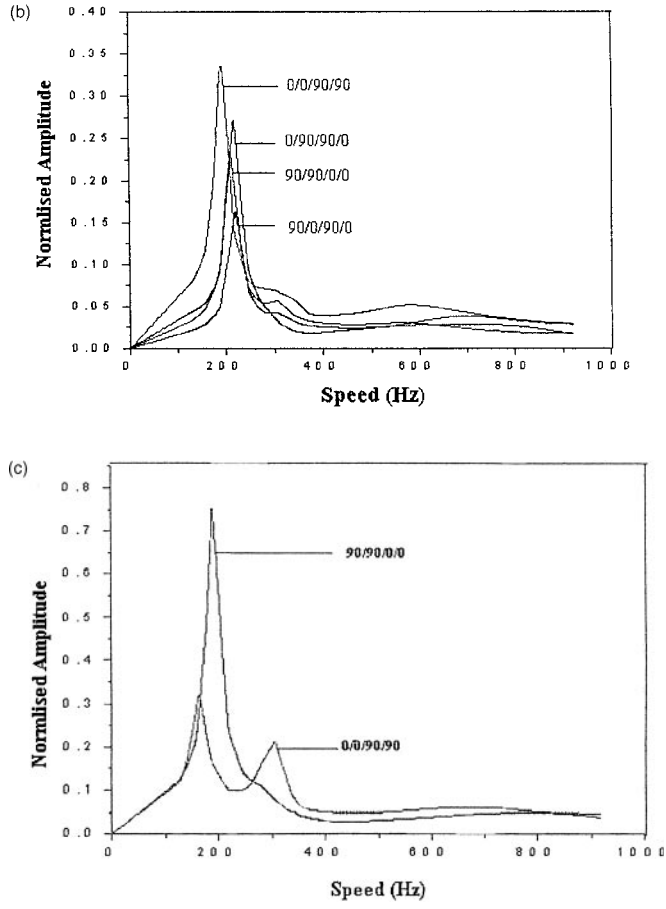

Figure 9. *(Continued).*

It has been noticed that the orientation of fibres influences a lot on the eigen frequencies. Both 90/0/90/0 and 90/90/0/0 stacking sequences stiffen the shafts. In the case of 90/90/0/0 stacking sequence, when crack depth increases the eigen frequencies are decreasing at a faster rate as compared to other stacking sequences for all the materials studied. Thus this stacking sequence is very sensitive to crack.

If the crack depth increases, the peak amplitude shifts towards the lower speed with a raise in peak amplitude. At higher crack depths the split of critical speeds are also observed in the response plots. Also, it has been noticed that the carbon–epoxy shafts are found to be less sensitive to the crack growth.

REFERENCES

1. Dimarogonas, A.D. (1970). *Dynamics Response of Cracked Rotors*, Technical Information Series, General Electric Co., Schenectady, New York.
2. Dimarogonas, A.D. and Paipetis, S.A. (1983). *Analytical Methods in Rotor Dynamics*, pp. 144–193, Applied Science, London.
3. Wauer, J. (1990). Dynamics of Cracked Rotors Literature Survey, *Applied Mechanics Reviews*, **43**: 13–17.
4. Gasch, R. (1993). A Survey of the Dynamic Behaviour of a Simple Rotating Shaft with a Transverse Crack, *J. Sound and Vibration*, **160**: 313–332.
5. Dimarogonas, A.D. (1996). Vibration of Cracked Structures: A State of the Art Review, *Engg. Fracture Mechanics*, **55**: 831–857.
6. Karabalis, D.L. and Bexos, D.E. (1983). Static, Dynamic and Stability Analysis of Structures Composed of Tapered Beam, *Computers and Structures*, **16**: 731–748.
7. Abramovich, H. and Livshits, A. (1994). Free Vibration of Non Symmetric Cross Ply Laminated Beams, *Journal of Sound and Vibration*, **176**(5): 597–612.
8. Kim, N.E. and Green, J.H. (1994). Sensitivity of Bonded and Composite Beams, *Journal of Sound and Vibration*, **177**(1): 71–92.
9. Chen, C.I. and Mucino, V.H. (1994). Flexible Rotating Beams Comparative Modelling of Isotropic and Composite Material Including Geometric Non-linearity, *Journal of Sound and Vibration*, **178**(5): 591–605.
10. Ramalingeswara Rao, S. and Ganesan, N. (1997). Dynamic Response of Non-uniform Composite Beams, *Journal of Sound and Vibration*, **200**(5): 563–577.
11. Krawczuk, M. and Ostachowicz, W.M. (1995). Modelling and Vibration Analysis of a Cantilever Composite Beam with Transverse Open Crack, *Journal of Sound and Vibration*, **183**(1): 69–89.
12. Zinberg, H. and Symmonds, M.F. (1970). The Development of an Advanced Composite Tail Rotor Drive Shaft, Presented at the 26th Annual National Forum of American Helicopter Society, Washington, DC, pp. 1–14.
13. Henriqúe dos Reis, L.M., Goldman, R.B. and Verstrate, P.H. (1987). Thin Walled Laminate Composite Cylindrical Tubes – Part 3, Critical Speed Analysis, *Journal of Composite Technology and Research*, **9**: 58–62.
14. Singh, S.P. and Gupta, K. (1996). Composite Shaft Rotor Dynamic Analysis Using Layerwise Theory, *Journal of Sound and Vibration*, **191**(5): 739–756.
15. Gupta, K. and Singh, S.P. (1998). Damping Measurements in Fibre Reinforced Composite Rotors, *Journal of Sound and Vibration*, **211**(3): 513–320.
16. Wettergren, H.L. (1997). The Influence of Imperfections on the Eigen Frequencies of a Rotating Composite Shaft, *Journal of Sound and Vibration*, **206**: 99–116.
17. Lim, Joon W. and Darlow, Mark S. (1996). Optimal Sizing of Composite Power Transmission Shafting, *Journal of the American Helicopter Society*, 75–83.
18. Belingardi, G., Calderate, P.M. and Rosetto, M. (1990). Design of Composite Material Drive Shafts for Vehicular Applications, *International Journal of Vehicle Design*, **11**: 553–563.
19. Salzar, Robert S. (1999). Design Considerations for Rotating Laminated Metal-matrix Composite Shafts, *Composites Science and Technology*, **59**: 883–896.
20. Sekhar, A.S. and Ravi Kumar, N. (September 1999). Vibrational Characteristics of Composite Shafts. In: *Proceedings of 17th Biennial ASME Vibrations Conference*, Las Vegas, Nevada, Paper No. DETC99/VIB-8277.